PROCEEDINGS OF SCIENCE

Determination of the gradient flow scale t_0 from a scale-setting approach combining Wilson and Wilson twisted mass valence quarks

Alejandro Saez,[a,*] **Alessandro Conigli,**[a,c,d] **Julien Frison,**[b] **Gregorio Herdoíza**[a] **and Carlos Pena**[a]

[a] *Department of Theoretical Physics, Universidad Autónoma de Madrid, 28049 Madrid, Spain and Instituto de Física Teórica UAM-CSIC, c/ Nicolás Cabrera 13-15 Universidad Autónoma de Madrid, 28049 Madrid, Spain*

[b] *ZPPT/NIC, DESY Zeuthen, Platanenallee 6, 15738 Zeuthen, Germany*

[c] *Helmholtz Institute Mainz, Johannes Gutenberg University, Mainz, Germany*

[d] *GSI Helmholtz Centre for Heavy Ion Research, Darmstadt, Germany*

E-mail: alejandro.saezg@uam.es

We perform a scale setting procedure of a mixed action setup consisting of valence Wilson twisted mass fermions at maximal twist on CLS ensembles with $N_f = 2 + 1$ flavours of $O(a)$-improved Wilson sea quarks. We determine the gradient flow scale t_0 using pion and kaon masses and decay constants in the isospin symmetric limit of QCD as external *physical* input. We provide an update for our results in [1] with ensembles at the physical pion mass and lattice spacings down to $a \approx 0.039$ fm. We employ model variation techniques to probe the systematic uncertainties in the extraction of the ground state signal of lattice observables, as well as for the continuum-chiral extrapolations used to determine t_0 at the physical point. We determine t_0 from a combination of the unitary Wilson lattice regularization and the mixed action regularization, which leads to an improved control of the systematic and statistical uncertainties.

European network for Particle physics, Lattice field theory and Extreme computing (EuroPLEx2023)
11-15 September 2023
Berlin, Germany

*Speaker

PoS(EuroPLEx2023)036

1. Introduction

The Standard Model of particle physics has been validated on numerous occasions through the corroboration of its theoretical predictions with corresponding experimental measurements. Nevertheless, it is expected that the Standard Model is merely an effective theory that is valid up to a specific energy scale. One of the primary objectives in contemporary fundamental physics is the search for physical phenomena that deviate from the Standard Model's predictions. One of the areas where new physics is anticipated to emerge is the quark-flavor sector of the Standard Model. In order to reduce the theoretical uncertainties on flavour observables and to uncover possible inconsistencies between theory and experiment, it is necessary to make precise theoretical determinations of the strong interaction effects. In this context, Lattice Field Theory represents the principal tool for calculating non-perturbative contributions to QCD from first principles.

We consider a mixed action lattice setup [2–7] aimed to address the leading systematic uncertainties affecting charm-quark observables. The mixed-action regularisation consists of Wilson twisted mass valence quarks combined with CLS ensembles with $O(a)$-improved Wilson sea quarks [13, 17]. The motivation behind employing this lattice regularisation is that when valence twisted mass fermions are tuned to maximal twist, an automatic $O(a)$ improvement can be achieved [4, 14], up to residual mass effects from u, d, s sea quarks. This is of particular relevance when working with heavy quarks. In this work we present an update of the use of this lattice formulation in the light (up/down) and strange quark sectors. This is a necessary step before studying heavy quark physics, since a matching between the valence quark masses and the $N_f = 2+1$ flavors in the sea is needed. Finally, we can carry out an independent computation of light-quark observables such as the pion and kaon decay constants and perform the scale setting using the gradient flow scale t_0 as an intermediate scale.

2. Sea-quark sector: $O(a)$-improved Wilson fermions

In the sea sector of our mixed action approach, we employ CLS gauge ensembles, which employ the Lüscher-Weisz gauge action with $N_f = 2+1$ non-perturbatively $O(a)$-improved Wilson quarks. The list of ensembles is reported in Table 1. These ensembles follow a chiral trajectory defined by a constant value of the trace of the sea quark mass matrix

$$\mathrm{Tr}\left(\mathrm{M_q}\right) = \mathrm{m_u} + \mathrm{m_d} + \mathrm{m_s} = \text{constant}, \tag{1}$$

which ensures that as the quark masses are varied for a fixed value of the inverse coupling β, the improved bare coupling $\tilde{g}_0$ is kept constant up to $O(a^2)$ effects. Since the condition in eq. (1) is defined in terms of the bare quark masses, we opt to follow a renormalized chiral trajectory by imposing that

$$\phi_4 = 8t_0\left(m_K^2 + \frac{1}{2}m_\pi^2\right) = 8t_0 m_K^2 + \frac{1}{2}\phi_2, \tag{2}$$

is kept fixed to its physical value. At LO in χPT this condition corresponds to keeping the sum of the renormalized quark masses fixed, since

$$\phi_4 \propto \mathrm{m_u^R} + \mathrm{m_d^R} + \mathrm{m_s^R}. \tag{3}$$

To impose this target chiral trajectory we perform a mass-shift of the simulated quark masses by Taylor expanding a lattice observable O in the bare quark masses [18] as follows

$$\left\langle O(m'_u, m'_d, m'_s)\right\rangle = \langle O(m_u, m_d, m_s)\rangle + \sum_q (m'_q - m_q)\frac{d\,\langle O\rangle}{dm_q}. \tag{4}$$

Following [23], we restrict to $q = s$ in the sum in eq. (4), since shifting only the strange quark mass leads to an improvement in the precision in the target observables. In order to determine the physical value of ϕ_4 to which the mass-shift is performed, an educated guess for the physical value of $t_0^{\rm ph}$ is needed. The value

$$\sqrt{t_0^{\rm guess}} = 0.1445(6)\ \text{fm}. \tag{5}$$

is selected as input. The specific value in eq. (5) is the outcome of the first steps of an *iterative* procedure which starts from an initial guess of t_0, chosen free of uncertainties, and that iterates the scale setting analysis, including correlations, until convergence to the value of t_0 is reached. Using the isospin symmetric (isoQCD) values of the pion and kaon meson masses recommended in Ref. [27],

$$m_\pi^{\rm isoQCD} = m_{\pi^0}^{\rm exp} = 134.9768(5)\ \text{MeV}, \tag{6}$$

$$m_K^{\rm isoQCD} = m_{K^0}^{\rm exp} = 497.611(13)\ \text{MeV}, \tag{7}$$

leads to the value for $\phi_4^{\rm guess} = 1.101(9)$.

3. Valence-quark sector: Wilson twisted mass fermions

The valence sector of our mixed action is composed of Wilson twisted mass (Wtm) fermions at maximal twist. The Wtm Dirac operator adds a chirally rotated mass term to the massless Wilson Dirac operator $D_{\rm W}$, which also includes the Sheikholeslami-Wohlert term,

$$D_{\rm Wtm} = D_{\rm W} + m_q^{(\rm v)} + i\gamma_5\mu_q^{(\rm v)}\ , \tag{8}$$

where the $m_q^{(\rm v)} = m_0^{(\rm v)} - m_{\rm cr}$ is the standard subtracted quark mass and $\mu_q^{(\rm v)}$ is the twisted mass parameter. Once the hopping parameter $\kappa^{(\rm v)} = (2am_0^{(\rm v)} + 8)^{-1}$ is tuned such that the light (u, d) valence PCAC quark mass vanishes ($m_{12}^{(\rm v)} = 0$) on each ensemble, physical observables computed form the Wtm Dirac operator are automatically $O(a)$-improved, save for residual effects coming from the sea sector which are $O(ag_0^4 \mathrm{Tr}\left(\mathrm{M_q}\right))$.

4. Matching sea and valence sectors

The use of a mixed action approach can lead to unitarity violations even in the continuum limit, provided the physical value of the quark masses in the sea and valence sectors are not tuned to the same value. We thus require a matching procedure to impose this condition, in addition to the tuning to maximal twist condition. To perform the former, we employ the observables ϕ_2, ϕ_4 defined in eq. (2), depending on the the kaon and pion masses,

$$\phi_2^{(\rm v)} \equiv \phi_2^{(\rm s)}\ , \quad \phi_4^{(\rm v)} \equiv \phi_4^{(\rm s)}. \tag{9}$$

β	a [fm]	id	m_π [MeV]	m_K [MeV]
3.40	0.086	H101	420	420
		H102	350	440
		H105	280	460
3.46	0.076	H400	420	420
		D450	222	480
3.55	0.064	N202	420	420
		N203	340	440
		N200	280	460
		D200	200	480
		E250	130	497
3.70	0.050	N300	420	420
		N302	340	440
		J303	260	470
		E300	176	496
3.85	0.039	J500	420	420
		J501	340	453

Table 1: $N_f = 2 + 1$ CLS ensembles [13, 17] used in the sea sector. These ensembles employ non-perturbatively $O(a)$-improved Wilson fermions and open boundary conditions in the time direction, except for ensembles E250 and D450, which employ periodic boundary conditions.

More specifically, we employ a set of measurements in the valence hyperplane $(\kappa^{(\mathrm{v})}, a\mu_l^{(\mathrm{v})}, a\mu_s^{(\mathrm{v})})$ that allows to perform small interpolations to the valence parameters so as to simultaneously satisfy eq. (9) as well as imposing the maximal twist condition, $m_{12}^{(\mathrm{v})} = 0$. The interpolation fit functions can be based on LO χPT. The matching procedure is illustrated in Fig. 1.

Once the valence parameters $(\kappa^{(\mathrm{v}),*},\ a\mu_l^{(\mathrm{v}),*},\ a\mu_s^{(\mathrm{v}),*})$ at which the matching and maximal twist conditions are satisfied, we interpolate the pion and kaon decay constants to the same *matching* point, as we will employ these observables to set the scale in the lattice.

Throughout the analysis, finite volume effects, which are found to be less than half a standard deviation for all observables and ensembles, are corrected using NLO χPT [25]. The extraction of the ground state signal of lattice observables is based on a model variation over the Euclidean time fit intervals.

5. Scale setting and determination of t_0^{ph}

To perform the scale setting, we employ a flavour averaged combination of the pion and kaon decay constants in units of t_0 [18]

$$\sqrt{8t_0} f_{\pi K} = \sqrt{8t_0} \times \frac{2}{3}\left(f_K + \frac{1}{2} f_\pi\right). \tag{10}$$

Up to logarithmic corrections, this quantity remains constant in SU(3) χPT at NLO along the renormalized chiral trajectory defined by $\phi_4 \equiv \phi_4^*$.

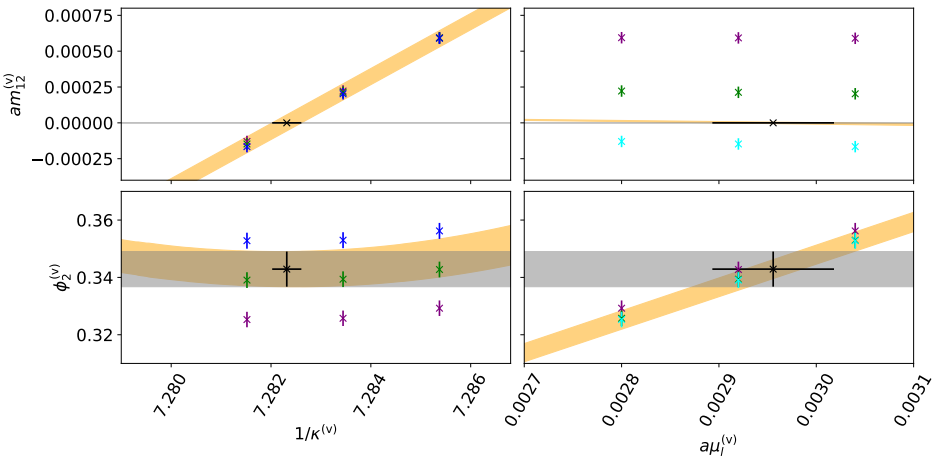

Figure 1: Top row: Light (u, d) valence PCAC quark mass from the valence *grid* of points – in the hyperplane of input parameters $(\kappa^{(v)}, a\mu_l^{(v)}, a\mu_s^{(v)})$ – interpolated to the maximal twist condition, $m_{12}^{(v)} = 0$. Bottom row: $\phi_2^{(v)}$ along the valence grid, interpolated to the sea value $\phi_2^{(s)}$. The sea sector parameters correspond to those of Table 1 for ensemble H105. The orange band in both figures represents the interpolation along the grid of valence parameters, while the horizontal grey line and band represent the target value to which we want to interpolate both observables. In the case of $am_{12}^{(v)}$, it is set to zero, and for $\phi_2^{(v)}$ to $\phi_2^{(s)}$. The interpolation of $\phi_4^{(v)}$ is not shown but it is carried out in a similar way to that of $\phi_2^{(v)}$.

For the scale setting, we consider three sets of data: (i) the *unitary* Wilson setup, which employs the same $O(a)$-improved Wilson Dirac operator in the sea and valence sectors. We refer to this case as "Wilson". (ii) the mixed action setup, once the matching of the sea and valence sectors has been performed, in addition to the tuning at maximal twist. This is referred to as "Wtm" case. (iii) the *Combined* set of data, in which the two previous sets are analysed together by imposing a common continuum limit result. More specifically, the "Wilson" and "Wtm" data sets can be analysed independently, leading to two determinations of the physical value of $t_0^{\rm ph}$. For the *Combined* case, a simultaneously fit of both data sets with independent sets of parameters characterising cutoff effects is performed. The lattice data can be parameterised as follows

$$\left(\sqrt{8t_0} f_{\pi K}\right)^{\rm latt} = \left(\sqrt{8t_0} f_{\pi K}\right)^{\rm cont} + c(a, \phi_2), \tag{11}$$

with $c(a, \phi_2)$ a function controlling cutoff effects. Several possible choices for the continuum behaviour and the cutoff effects are explored. For the continuum mass-dependence we consider SU(3) χPT expressions at NLO

$$\left(\sqrt{8t_0} f_{\pi K}\right)^{\rm cont} = \frac{p_1}{8\pi\sqrt{2}} \left[1 - \frac{7}{6} L\left(\frac{\phi_2}{p_1^2}\right) - \frac{4}{3} L\left(\frac{\phi_4 - \phi_2/2}{p_1^2}\right) - \frac{1}{2} L\left(\frac{4\phi_4/3 - \phi_2}{p_1^2}\right) + p_2 \phi_4\right] , \tag{12}$$

where, $L(x) = x \log(x)$.

One can also consider SU(2) χPT expressions at NLO

$$\left(\sqrt{8t_0}f_{\pi K}\right)^{\text{cont}} = p_2 + p_3\phi_2 + p_4\phi_4 - \left(p_5 + \frac{p_1}{6\pi}\right) L\left(\frac{\phi_2}{p_1^2}\right). \tag{13}$$

Another alternative is to employ a Taylor expansion around the symmetric point ϕ_2^{sym} to the second order,

$$\left(\sqrt{8t_0}f_{\pi K}\right)^{\text{cont}} = p_1 + p_2(\phi_2 - \phi_2^{\text{sym}})^2, \tag{14}$$

or to the fourth order

$$\left(\sqrt{8t_0}f_{\pi K}\right)^{\text{cont}} = p_1 + p_2(\phi_2 - \phi_2^{\text{sym}})^2 + p_3(\phi_2 - \phi_2^{\text{sym}})^4. \tag{15}$$

To characterise the lattice spacing dependence, we consider

$$c(a,\phi_2) = c_1\frac{a^2}{t_0} + c_2\phi_2\frac{a^2}{t_0} + c_3\alpha_s^{\hat{\Gamma}}\frac{a^2}{t_0}, \tag{16}$$

and we consider the effect of switching on/off the different c_i's. A exploratory study of the impact of including logarithmic corrections of $O(a^2\alpha_s^{\hat{\Gamma}})$ considering the smallest value of the anomalous dimensions $\hat{\Gamma}$ reported in [28] is also incorporated in the analysis by including the c_3 term while setting $c_1 = 0$. We explored other values of $\hat{\Gamma}$ but no sensitivity to this change was found with the set of ensembles under analysis and the set of values of $\hat{\Gamma}$ considered.

In addition to a variation of the functional forms, we explore the possibility of performing cuts in the data, by removing the coarsest lattice spacing $\beta = 3.40$, the second coarsest $\beta = 3.46$, the symmetric point ensembles with $m_\pi = 420$ MeV, the second heaviest pion masses ensembles $m_\pi = 360$ MeV, spatial volumes $m_\pi L < 4.1$ or the double cut $\beta = 3.40$ & $m_\pi = 420$ MeV.

The correlations present in the Monte Carlo data are retained throughout the analysis. In the chiral-continuum fit, the χ^2 function includes the correlations among the $\sqrt{t_0}f_{\pi K}$ data points while the residual cross-correlations between $\sqrt{t_0}f_{\pi K}$ and ϕ_2 is neglected in the fit. We observe, however, that this leads to a tiny deviation of the expectation value of the chi-squared [21], $\langle\chi^2\rangle$, away from the number of degree-of-freedom, i.e. the expected value when considering a correlated fit.

To study the systematic effects associated with model variation in the chiral and continuum extrapolations, we use the model averaging method introduced in [19] with the information criterion proposed in [20] to take into account fits that are not fully correlated. According to this information criterion, each fit model is assigned a weight

$$W \propto \exp\left(-\frac{1}{2}\left(\chi^2 - 2\langle\chi^2\rangle\right)\right), \tag{17}$$

which allows to compute a weighted average for $\sqrt{t_0}f_{\pi K}$ over the explored models. The method also assigns a systematic uncertainty coming from the model variation. [1] This model averaging procedure tends to penalize models with cuts in data and large number of fit parameters. In our case, we observe that our lattice data is well described by the fit forms explored without performing any

[1] We have also considered this model averaging technique to extract the ground state signal of the relevant lattice observables by scanning over Euclidean time fit intervals.

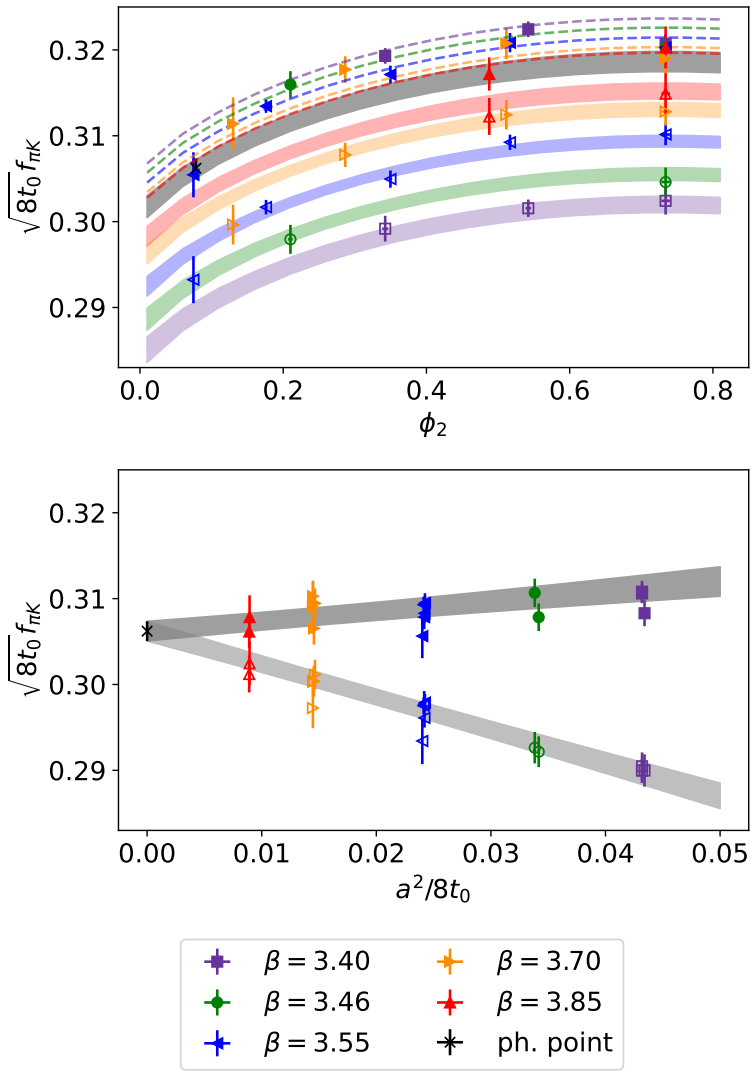

Figure 2: Chiral and continuum extrapolations of $\sqrt{8t_0}f_{\pi K}$. We show the measurements for Wilson (empty points) and Wtm (filled points). The fit form in eq. (12) is used for mass dependence together with eq. (16) with $c_2 = c_3 = 0$ to parameterise the lattice spacing dependence. No cuts are applied in this specific fit. Points with the same colour refer to a common value of the lattice spacing. The grey band represents the continuum limit dependence for the *Combined* data set analysis, while the coloured bands represent the chiral fits at each lattice spacing for the Wilson data, and, similarly, the dashed lines (without showing uncertainty in the fits) correspond to the Wtm case. *Bottom*: dependence of $\sqrt{8t_0}f_{\pi K}$ on the lattice spacing. All points are projected to physical pion mass using the fit result to eq. (12), and the continuum extrapolation is done fitting to eq. (16). The modification of the weight of the χ^2 function in eq. (18) acting on the $\beta = 3.40$ and $m_\pi = 420$ MeV data was included. The p-value for this model is 0.55 and it is one of the models contributing most to the model average.

cut in the data, which results in a large penalization by the TIC for models which cut the coarsest lattice spacing $\beta = 3.40$ and heaviest pion mass $m_\pi = 420$ MeV. In order to counteract for this effect, we introduce a systematic error contribution in the definition of the χ^2 of the fits for these set of esembles in a similar manner as what was done in [30]. More specifically, the matrix elements of the weight matrix $\mathcal{W}$ in the χ^2 function are modified to include terms associated to systematic uncertainties. In the case of a diagonal weight matrix,

$$\mathcal{W}_i^{-1} = \sigma_i^2 + c_\beta^2 \left(\frac{a^2}{8t_0}\right)^4 + c_{\phi_2}^2 \phi_2^4. \tag{18}$$

In the the first term in the rhs, σ_i, is the statistical error of the i-th data point. The coefficients c_β and c_{ϕ_2} are chosen such that the elements of the weight matrix $\mathcal{W}$ for ensembles at the symmetric point or at the coarsest lattice spacing, are no longer significantly enhanced with respect to those lying closer to the continuum or at the physical pion mass. This ensures that the chiral-continuum extrapolation is not dominated by ensembles with the heaviest pion masses and farther away from the continuum, which tend to have smaller uncertainties than physical point ensembles or ensembles with very fine values of a. By informing the χ^2 about the fact that the effective theories used to characterize the lattice spacing and the light quark mass dependence work best at smaller values of a and m_π, respectively, the weights of the model average are more evenly distributed between the different data cuts. The model variation procedure and the corresponding model average are illustrated in Fig. 3, while the specific model based on eq. (12) for the continuum behaviour and $c_2 = c_3 = 0$ term in eq. (16) is shown in Fig. 2.

Once $\sqrt{8t_0} f_{\pi K}$ is determined at the physical point (i.e. continuum limit result with physical pion and kaon masses), using a prescription for the isoQCD values of the pion and kaon decay constants [27]

$$f_\pi^{\text{isoQCD}} = 130.56(13) \text{ MeV}, \quad f_K^{\text{isoQCD}} = 157.2(5) \text{ MeV}, \tag{19}$$

as physical inputs, it is possible to determine the physical value of the gradient flow scale t_0^{ph}. Our results for the three types of analysis (Wilson, Wtm and Combined), together with a comparison with other studies also based on $N_f = 2 + 1$ CLS ensembles, are presented in Fig. 4. We observe a shift of the central value of t_0 depending on whether the physical inputs of FLAG21 [27] or FLAG16 [26] are considered, the latter case giving results with bigger values of t_0.

6. Conclusions

We have presented an update of a scale setting procedure based on physical inputs for the pion and kaon decay constants, using a mixed action consisting of twisted mass valence quarks on CLS $O(a)$-improved sea quarks [29] with ensembles at the physical pion mass and lattice spacing down to $a \approx 0.039$ fm. We have explored the systematic effects associated to model variation in the chiral and continuum limits, and demonstrated the effectiveness of combining the Wilson and mixed action (Wtm) calculations to improve the precision of t_0. The current effort to extend this work is to employ $SU(2)$ ChPT to perform the chiral extrapolation of $\sqrt{8t_0} f_\pi$, thus using only physical input for the pion decay constant. With respect to f_K, the extraction of the pion decay constant f_π from the leptonic decay rate is less sensitive to QED corrections, and furthermore the

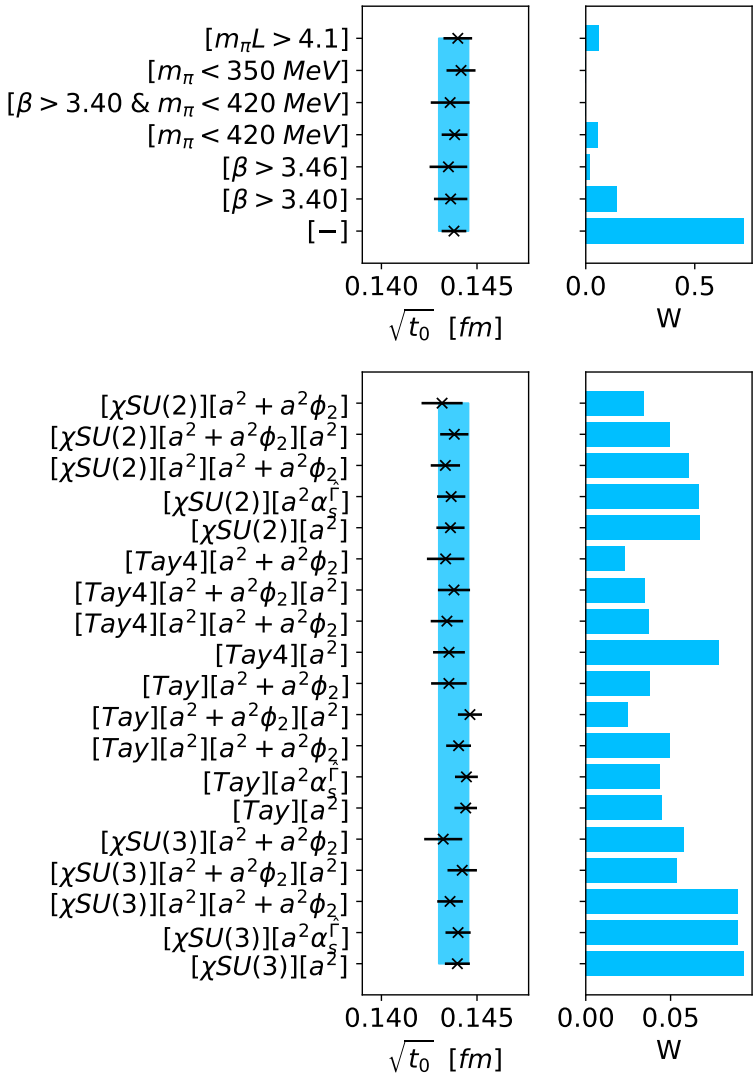

Figure 3: Model average results for the determination of $\sqrt{t_0}$ at the physical point using the combined analysis of both Wilson and Wtm results and $f_{\pi K}$ as physical input. *Top*: model average over cuts in the data. The model weights W are given by eq. (17). For each label of the cut performed to the data displayed in the panel, an average according to the model weights was taken over the various fit forms employed to perform the chiral-continuum extrapolation. The label "[-]" refers to doing no cut in data. In all models the systematic term of eq. (18) was included in the definition of the χ^2, so even in the "[-]" models points at the coarsest lattice spacing, $\beta = 3.40$, and heaviest pion mass, $m_\pi = 420$ MeV, are penalized in the fit. *Bottom*: model average over different fit functions to perform the chiral-continuum extrapolation. When two different labels are used for the cutoff effects, the first refers to the ones used in the Wilson data and the second to the ones used in the Wtm. If only one label is present, it implies that the same cutoff effects were used, but with different fit parameters. For each label of the fit form displayed in the panel, an average was taken over the various data cuts according to the model weights. The blue vertical band shows the total model average result with systematic and statistical uncertainties added in quadrature. All p-values computed following [21] for each individual model are found to be greater than 0.1. Label $[\chi SU(2)]$ refers to eq. (13), $[\chi SU(3)]$ to eq. (12), $[Tay]$ to eq. (14), $[Tay4]$ to eq. (15), $[a^2]$ to using eq. (16) for the cutoff effects with $c_2 = c_3 = 0$, $[a^2 + a^2\phi_2]$ refers to setting $c_3 = 0$, and $[a_2\alpha_S^\Gamma]$ refers to setting $c_1 = c_2 = 0$.

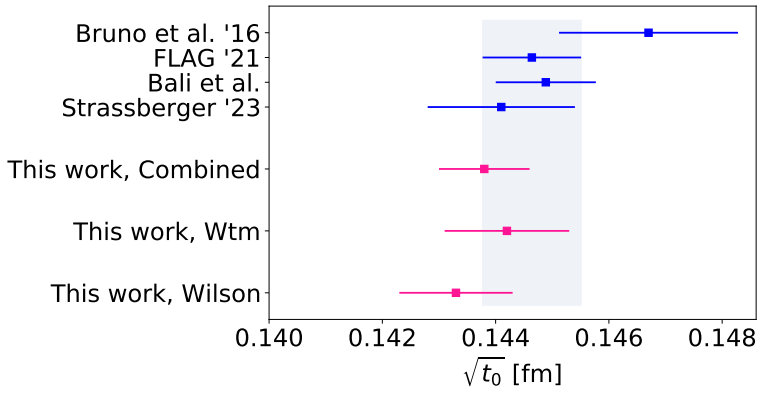

Figure 4: Results for the gradient flow scale $\sqrt{t_0}$ in physical units based on the model average (pink points) for our three types of analysis (Wilson, Wtm and Combined), compared with the $N_f = 2 + 1$ FLAG average [27] and with other determinations also based on $N_f = 2 + 1$ CLS ensembles (blue points). In Bruno et al. [18] the FLAG16 [26] prescription was used to define the physical input. Strassberger [23] use FLAG21 [27] physical input, as we have done in this study. Together with the inclusion of additional ensembles in the analysis, we observe that the use of FLAG21 physical input tends to reduce the value of $\sqrt{t_0}$ with respect to FLAG16.

uncertainty from the CKM matrix element CKM $|V_{ud}|$ is smaller than that from $|V_{us}|$. In addition, the updated determination of t_0 will be applied to the calculation of light quark masses and to our charm physics project based on this mixed-action approach [9–11].

Acknowledgements

We are grateful to our colleagues in the Coordinated Lattice Simulations (CLS) initiative for the generation of the gauge field configuration ensembles employed in this study. We acknowledge PRACE for awarding us access to MareNostrum at Barcelona Supercomputing Center (BSC), Spain and to HAWK at GCS@HLRS, Germany. The authors thankfully acknowledge the computer resources at MareNostrum and the technical support provided by Barcelona Supercomputing Center (FI-2020-3-0026). We thank CESGA for granting access to Finis Terrae II. This work is partially supported by grants PGC2018-094857-B-I00 and PID2021-127526NB-I00, funded by MCIN/AEI/10.13039/501100011033 and by "ERDF A way of making Europe", and by the Spanish Research Agency (Agencia Estatal de Investigaci´on) through grants IFT Centro de Excelencia Severo Ochoa SEV-2016-0597 and No CEX2020-001007-S, funded by MCIN/AEI/10.13039/501100011033. We also acknowledge support from the project H2020-MSCAITN-2018-813942 (EuroPLEx), under grant agreementNo. 813942, and the EU Horizon 2020 research and innovation programme, STRONG-2020 project, under grant agreement No 824093.

References

[1] A. Saez, A. Conigli, J. Frison, G. Herdoiza, C. Pena, "Determination of the Gradient Flow Scale t_0 from a Mixed Action with Wilson Twisted Mass Valence Quarks", arXiv:2401.11546 [hep-lat].

[2] A. Bussone *et al.* [Alpha], Eur. Phys. J. C **84** (2024) no.5, 506 doi:10.1140/epjc/s10052-024-12816-4 [arXiv:2309.14154 [hep-lat]].

[3] G. Herdoíza, C. Pena, D. Preti, J. Á. Romero and J. Ugarrio, "A tmQCD mixed-action approach to flavour physics", EPJ Web Conf. 175 (2018), 13018, [arXiv:1711.06017 [hep-lat]].

[4] A. Bussone et al. [ALPHA], "Heavy-quark physics with a tmQCD valence action", PoS LATTICE2018 (2019), 270, [arXiv:1812.01474 [hep-lat]].

[5] J. Ugarrio et al. [Alpha], "First results for charm physics with a tmQCD valence action", PoS LATTICE2018 (2018), 271, [arXiv:1812.05458 [hep-lat]].

[6] A. Bussone et al. [ALPHA], "Matching of $N_f = 2 + 1$ CLS ensembles to a tmQCD valence sector", PoS LATTICE2018 (2019), 318, [arXiv:1903.00286 [hep-lat]].

[7] J. Frison et al., "Heavy semileptonics with a fully relativistic mixed action", PoS LATTICE2019 (2019), 234, [arXiv:1911.02412 [hep-lat]].

[8] G. Herdoiza et al., PoS LATTICE2022 (2022), 268.

[9] A. Bussone, A. Conigli, J. Frison, G. Herdoiza, C. Pena, D. Preti, A. Saez, J. Ugarrio, "Hadronic physics from a Wilson fermion mixed-action approacg: Charm quark mass and $D_{(s)}$ meson decay constants", [arXiv:2309.14154].

[10] A. Conigli et al., PoS LATTICE2022 (2022), 235.

[11] J. Frison et al., PoS LATTICE2022 (2022), 378.

[12] M. Lüscher and S. Schaefer, "Lattice QCD without topology barriers", JHEP 07 (2011), 036, [arXiv:1105.4749 [hep-lat]].

[13] M. Bruno et al., "Simulation of QCD with $N_f = 2 + 1$ flavors of non-perturbatively improved Wilson fermions", JHEP 02 (2015), 043, [arXiv:1411.3982 [hep-lat]].

[14] R. Frezzotti and G. C. Rossi, JHEP 08 (2004), 007, doi:10.1088/1126-6708/2004/08/007, [arXiv:hep-lat/0306014 [hep-lat]].

[15] R. Frezzotti et al. [Alpha], "Lattice QCD with a chirally twisted mass term", JHEP 08 (2001), 058, [arXiv:hep-lat/0101001 [hep-lat]].

[16] C. Pena, S. Sint and A. Vladikas, "Twisted mass QCD and lattice approaches to the Delta I=1/2 rule", JHEP 09 (2004), 069, [arXiv:hep-lat/0405028 [hep-lat]].

[17] D. Mohler, S. Schaefer and J. Simeth, "CLS 2+1 flavor simulations at physical light- and strange-quark masses", EPJ Web Conf. 175 (2018) 02010, [1712.04884].

[18] M. Bruno, T. Korzec and S. Schaefer, "Setting the scale for the CLS 2 + 1 flavor ensembles," Phys. Rev. D **95** (2017) no.7, 074504, doi:10.1103/PhysRevD.95.074504, [arXiv:1608.08900 [hep-lat]].

[19] William I. Jay and Ethan T. Neil, "Bayesian model averaging for analysis of lattice field theory results", Phys. Rev. D **103**, 114502 (2021), doi:10.1103/PhysRevD.103.114502, [arXiv:2008.01069].

[20] J. Frison, "Towards fully bayesian analyses in Lattice QCD", [arXiv:2302.06550].

[21] Mattia Bruno and Rainer Sommer, "On fits to correlated and auto-correlated data", [arXiv:2209.14188].

[22] Jochen Heitger, Fabian Joswig, Simon Kuberski, "Determination of the charm quark mass in lattice QCD with 2+1 flavours on fine lattices", JHEP 2021, 288 (2021), [arXiv:2101.02694].

[23] B. Straßberger, "Towards Higher Precision Lattice QCD Results: Improved Scale Setting and Domain Decomposition Solvers," doi:10.18452/26517

[24] G. S. Bali *et al.* [RQCD], "Scale setting and the light baryon spectrum in $N_f = 2 + 1$ QCD with Wilson fermions," JHEP **05** (2023), 035 doi:10.1007/JHEP05(2023)035 [arXiv:2211.03744 [hep-lat]].

[25] Gilberto Colangelo and Stephan Durr and Christoph Haefeli, "Finite volume effects for meson masses and decay constants", [arXiv:hep-lat/0503014].

[26] S. Aoki *et. al*, "Review of lattice results concerning low-energy particle physics", [arXiv:1607.00299].

[27] Y. Aoki *et. al*, "FLAG Review 2021", Eur.Phys.J.C 82 (2022) 10, 869, doi:10.1140/epjc/s10052-022-10536-1, [arXiv:hep-lat/2111.09849].

[28] Nikolai Husung, "Logarithmic corrections to $O(a)$ and $O(a^2)$ effects in lattice QCD with Wilson or Ginsparg-Wilson quarks", [arXiv:hep-lat/2206.03536].

[29] A. Saez, A. Conigli, J. Frison, G. Herdoiza, C. Pena and J. Ugarrio, PoS **LATTICE2022** (2023), 357 doi:10.22323/1.430.0357

[30] Dalla Brida, Mattia and Fritzsch, Patrick and Korzec, Tomasz and Ramos, Alberto and Sint, Stefan and Sommer, Rainer, "Slow running of the Gradient Flow coupling from 200 MeV to 4 GeV in $N_f = 3$ QCD", [arXiv:hep-lat/1607.06423]. doi:10.1103/PhysRevD.95.014507